J|A|C|S
ARTICLES
Published on Web 10/27/2006

Thin Film Voltammetry of Spinach Photosystem II. Proton-Gated Electron Transfer Involving the Mn_4 Cluster

Khrisna Alcantara,[†] Bernard Munge,[†,‡] Zeus Pendon,[†] Harry A. Frank,[†] and James F. Rusling*[,†,§]

Contribution from the Department of Chemistry, University of Connecticut, Storrs, Connecticut 06269-3060, and Department of Pharmacology, University of Connecticut Health Center, Farmington, Connecticut 06032

Received June 27, 2006; E-mail: James.Rusling@uconn.edu

Abstract: Thin film voltammetry was used to obtain direct, reversible, electron-transfer peaks between electrodes and the spinach photosystem II (PS II) reaction center in lipid films for the first time. Three well-defined pairs of reduction−oxidation peaks were found using cyclic and square wave voltammetry at 4 °C at pH 7.5, reflecting direct, reversible electron transfer involving cofactors of PS II. These peaks were assigned to the oxygen-evolving complex (OEC) tetramanganese cluster (E_m = 0.2 V vs NHE), quinones (E_m = −0.29 V), and pheophytin (E_m = −0.72 V). PS II that was depleted of the OEC did not give the peak at 0.2 V. Observed E_m values, especially for the OEC, may be influenced by protein−lipid interactions and electrode double-layer effects. Voltammetry at pH 6 and at pH 7.5 with a time window of >100 ms revealed that the manganese cluster oxidation is gated by slow deprotonation of a reduced form. Additional rapid protonation/deprotonation steps are also involved in the electrochemical reduction−oxidation pathways.

Introduction

Photosystem II (PS II) is a large transmembrane protein−cofactor complex that facilitates the conversion of photons into chemical energy in higher plants, algae, and cyanobacteria by catalyzing light-driven oxidation of water to oxygen and reduction of plastoquinone.[1−3] Light-harvesting pigments in PS II deliver energy to the primary electron donor (P680), a chlorophyll dimer. Photoexcitation converts P680 to P680*, initiating a series of one-electron-transfer steps (Scheme 1). The primary electron acceptor is pheophytin (Pheo), while subsequent electron acceptors include plastoquinones A (Q_A) and B (Q_B). Direct electron ejection from P680* yields $P680^+$. Electron donation to $P680^+$ then occurs from redox-active tyrosine (Y_Z) that works in concert with a tetramanganese (Mn_4) cluster to oxidize H_2O and produce molecular oxygen.[2,4] Recent X-ray crystal structures[5,6] of PS II from cyanobacteria, the most recent addressing previously unseen cofactors at 3.0 Å resolution,[6d] provide significant insight into the molecular arrangement of the multiple subunits. Perhaps more important for our present work, recent time-resolved X-ray absorption studies of spinach PS II elucidated oxidation state, structural, and protonation changes in the Mn_4 cluster[7−9] that can be used to aid in the interpretation of electrochemical data that we present below.

Scheme 1. Electron-Transfer Pathways for PS II Showing Approximate Midpoint Potentials (vs SHE) for the Various Redox Centers in PS II and Estimated Time Scales for Redox Events[a]

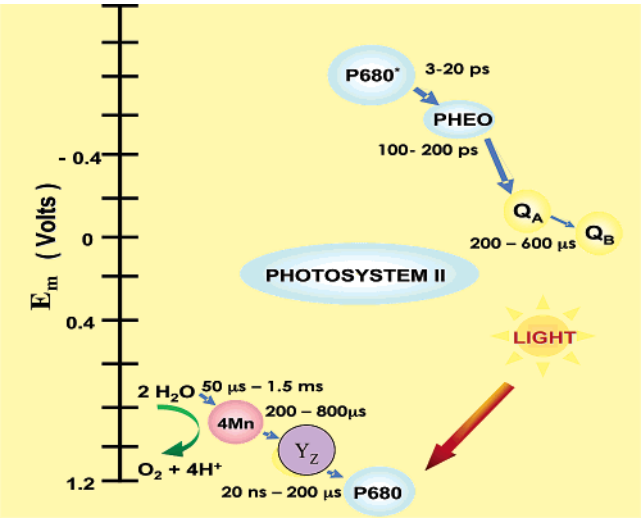

[a] Key redox centers include P680, pheophytin, quinone A, and quinone B. Adapted from ref 11. See Table 1 for source references.

[†] University of Connecticut.

[‡] Present address: Chemistry Department, Salve Regina University, Newport, RI 02840.

[§] University of Connecticut Health Center.

(1) Diner, B. A.; Babcock, G. T. In *Oxygenic Photosynthesis*: *The Light Reactions*; Ort, D. R., Yocum, C. F., Eds.; Kluwer Academic Publishers: Dordrecht, The Netherlands, 1996; pp 213−247.
(2) Britt, R. D. In *Oxygenic Photosynthesis: The Light Reactions*; Ort, D. R., Yocum, C. F., Eds.; Kluwer Academic Publishers, Dordrecht, The Netherlands, 1996; pp 137−164.
(3) Nugent, J. H. A. *Eur. J. Biochem.* **1996**, *237*, 519−531.
(4) Witt, H. T. *Phys. Chem. Chem. Phys.* **1996**, *100*, 1923−1942.
(5) Zouni, A.; Witt, H.-T.; Keru, J.; Fromme, P.; Krauss, N.; Saenger, W.; Orth, P. *Nature (London)* **2001**, *409*, 739−743.
(6) (a) Kamiya, N.; Shen, J.-R. *Proc. Natl. Acad. Sci. U.S.A.* **2003**, *100*, 98−103. (b) Ferreira, K. N.; Iverson, T. M.; Maghlaoui, K. Barber, J.; Iwata, S. *Science* **2004**, *303*, 1831−1838. (c) Liu, Z.; Yan, H.; Wang, K.; Kuang, T.; Zhang, T.; Gui, L.; An, X.; Chang, W. *Nature (London)* **2004**, *428*, 287−292. (d) Loll, B.; Kern, J.; Saenger, W.; Zouni, A.; Biesiadka, J. *Nature (London)* **2004**, *438*, 1040−1044.
(7) Dau, H.; Iuzzolino, L.; Dittmer, J. *Biophys. Biochim. Acta* **2001**, *1503*, 24−39.

10.1021/ja0645537 CCC: $33.50

Knowledge of the redox properties of protein-bound cofactors and the influence of the microenvironment and structural modifications of PS II are key to understanding how photosynthetic reaction center (RC) proteins achieve efficient electron transport across biological membranes. Directly addressing plant photosystem proteins electrochemically represents a major challenge that could pay off in detailed fundamental characterization of redox processes involving cofactors in the electron-transfer pathways of these proteins. Nature utilizes membranes with embedded proteins incorporating redox cofactors to shuttle electrons to critical sites that support life processes. Mimicking the membrane superstructures containing RC proteins on electrodes offers a powerful approach to explore their redox chemistry in biomimetic microenvironments.[10]

Thin film voltammetry has become a valuable approach for studying the redox properties and reactions of proteins and enzymes.[10−13] In this technique, proteins are trapped in monolayer or multilayer films on electrode surfaces, often using molecular coadsorbates, polyions, or insoluble lipids as "glue". The resulting high concentration of protein directly on the electrode surface can give much larger and more well-defined voltammetric peaks than for the same proteins in solution. This approach eliminates the influence of diffusion of large membrane proteins such as PS I and II, which can render signals unobservable for the proteins in solution.

Immobilization of photosynthetic RC proteins on metal electrodes or between capacitor plates has been reported previously. That work involved measuring photocurrents or photovoltages,[14] investigating electric-field effects on light-induced charge separation,[15] and obtaining surface-enhanced Raman spectra.[16] The photocatalytic activity of solubilized cyanobacterial PS I in an electron-transfer chain including cytochrome c_6 and methyl viologen has been measured by voltammetry of cytochrome c_6, enabling rate constant measurements for reaction with photoactivated PS I.[17] Cliffel et al. have studied the effect of surface chemistry on adsorption of spinach PS I on electrodes coated with self-assembled monolayers (SAMs) of organothiols.[18] They later used this information to deposit PS I on SAM electrodes[19] and imaged patterned PS I electrodes with scanning electrochemical microscopy.

Our goal in the present study was to obtain direct voltammetry of bound redox cofactors in PS II in lipid films in the absence of light to investigate their redox mechanisms. We previously measured direct reversible voltammetry of two cofactors bound to spinach PS I protein in thin lipid films, reported apparent electrochemical electron-transfer rate constants, and observed reactions of the terminal electron acceptors of PS I with its natural redox partner ferredoxin in solution.[20] We also reported irreversible voltammetry for redox cofactors in the reaction center of the purple bacterium *Rhodobactor sphaeroides* and its reaction with reduced cytochrome *c* (cyt *c*) in solution.[21] It is important to realize that midpoint potentials measured from the voltammograms can be influenced significantly by lipid−protein interactions and electrical double-layer effects.[13] Thus, the main value of the approach resides in gaining mechanistic insight into redox processes, which is our focus here.

In this paper, we present direct thin film voltammetry of spinach PS II in lipid films on electrodes for the first time. At a midpoint potential of −0.29 V vs NHE by cyclic voltammetry (CV) at pH 7.5, we found chemically reversible oxidation−reduction peaks that we assigned to quinone cofactors. A second pH-dependent reduction peak found at 0.2 V at pH 7.5 was assigned to the oxygen-evolving manganese cluster (Mn_4) by comparison with cyclic voltammograms of Mn-depleted PS II. The dependence of the Mn_4 cluster electrochemistry in PS II on the pH and voltammetric time window revealed an unusual proton-gated electron-transfer process.

Experimental Section

Materials. Dimyristoylphosphatidylcholine (DMPC; >99%) was from Sigma. A 5.3 mM DMPC dispersion was ultrasonicated for 4 h to obtain vesicles.[13] Water was purified with a Hydro Nanopure system to a specific resistivity of >16 mΩ cm.

Preparation of PS II RCs. Berthold et al. described a method for the isolation of an oxygen-evolving PS II preparation[22] active in the reconstitution of electron-transport pathways that are known to occur in unfractionated membranes.[23] Procedures for the preparation of thylakoid membranes from spinach and the BBY particles from the spinach thylakoid were described previously.[24] A BBY particle dispersion having a chlorophyll (Chl) concentration of 2 mg/mL was mixed with an equal volume of 2% dodecyl β-maltoside (β-DM) and incubated for 5 min on ice. The mixture was centrifuged at 18000*g* using an SS34 rotor. The supernatant was applied in 1 mL aliquots onto the top of the centrifuge tubes of the SW40 rotor containing a 0.1−1.0 M sucrose gradient with 10 mM HEPES and 0.06% β-DM at pH 7.6 and centrifuged at 285000*g* for 23 h. The chlorophyll *b*-free fourth band (from the top) containing the PS II reaction center was collected, and

(8) Haumann, M.; Müller, C.; Liebisch, P.; Iuzzolino, L.; Dittmer, J.; Grabolle, M.; Neisius, T.; Meyer-Klaucke, W.; Dau, H. *Biochemistry* **2005**, *44*, 1894−1908.

(9) Haumann, M.; Liebisch, P.; Müller, C.; Barra, M,; Grabolle, M.; Dau, H. *Science* **2005**, *310*, 1019−1020.

(10) (a) Rusling J. F.; Zhang, Z. In *Handbook of Surfaces and Interfaces of Materials, Vol. 5, Biomolecules, Biointerface, and Applications*; Nalwa, H. S., Ed.; Academic Press: San Diego, 2001; pp 33−71. (b) Rusling, J. F.; Zhang, Z. In *Biomolecular Films*; Rusling, J. F., Ed.; Marcel Dekker: New York, 2003; pp 1−64.

(11) Hill. R.; Bendall, F. *Nature* **1960**, *186*, 136−138.

(12) (a) Armstrong, F. A.; Heering, H. A.; Hirst, J. *Chem. Soc. Rev.* **1997**, *26*, 169−179. (b) Armstrong, F. A. In *Bioelectrochemistry of Biomacromolecules*; Lenaz G., Milazzo G., Eds.; Birkhauser Verlag: Basel, Switzerland, 1997; pp 205−255. (c) Armstrong F. A.; Wilson, G. S. *Electrochim. Acta* **2000**, *45*, 2623−2645. (d) Niki, K.; Gregory, B. W. In *Biomolecular Films*; Rusling, J. F., Ed.; Marcel Dekker: New York, 2003; pp 65−98. (e) Léger, C. L.; Elliot, S. J.; Hoke, K. R.; Jeuken, L. J. C.; Jones, A. K.; Armstrong, F. A. *Biochemistry* **2003**, *42*, 8653−8662.

(13) Rusling, J. F. *Acc. Chem. Res.* **1998**, *31*, 363−369

(14) For examples see: (a) Lee, I.; Lee, J. W.; Warmack, R. J.; Allison, D. P.; Greenbaum. E. *Proc. Natl. Acad. Sci. U.S.A.* **1995**, *92*, 1965−1969. (b) Lee, J. W.; Lee, I.; Greenbaum. E. *Biosens. Bioelectron.* **1996**, *11*, 375−387 and references therein. (c) Lee, I.; Lee, J. W.; Greenbaum. E. *Phys. Rev. Lett.*. **1997**, *79*, 3294−3297. (d) Yasuda, Y.; Kawakami, Y.; Toyotama, H. *Thin Solid Films* **1997**, *292*, 198−191. (e) Lee, I.; Lee, J. W.; Stubna, A.; Greenbaum. E. *J. Phys. Chem. B* **2000**, *104*, 2439−2443.

(15) Moser, C. C.; Sension, R. J.; Szarka, A. Z.; Repinec, S. T.; Hochstrasser, R. M.; Dutton, P. L. *Chem. Phys.* **1995**, *197*, 343−354.

(16) (a) Picorel, R.; Holt, R, E.; Heald, R.; Cotton, T. M.; Seibert, M. *J. Am. Chem. Soc.* **1991**, *113*, 2839−2843. (b) Picorel, R.; Chumanov, G.; Montoya, G.; Cotton, T. M.; Toon, S.; Seibert, M. *J. Phys. Chem.* **1994**, *98*, 6017−6022.

(17) Proux-Delrouyre, V.; Demaille, C.; Leibl, W.; Sétif, P.; Bottin, H.; Bourdillon, C. *J. Am. Chem. Soc.* **2003,** *125*, 13686−13692.

(18) Ko, S. B.; Babcock. B.; Jennings, G. K.; Tilden, S. G.; Peterson, R. R.; Cliffel, D. *Langmuir* **2004**, *20*, 4033−4038.

(19) (a) Ciobanu, M.; Kincaid, H. A.; Jennings, G. K.; Cliffel, D. E. *Langmuir* **2005**, *21*, 692−698. (b) Kincaid, H. A.; Niedringhaus, T.; Ciobanu, M.; Cliffel, D. E.; Jennings, K. G. *Langmuir* **2006**, *22*, 8114−8120.

(20) Munge, B.; Kumar, D. S.; Robielyn, I.; Pendon, Z.; Frank, H. A.; Rusling, J. F. *J. Am. Chem. Soc.* **2003,** *125*, 12457−12463.

(21) Munge, B.; Pendon, Z.; Frank, H. A.; Rusling, J. F. *Bioelectrochemistry* **2001**, *54*, 145−150.

(22) Berthold, D. A.; Babcock, G. T.; Yocum, C. F. *FEBS Lett.* **1981**, *134*, 231−234.

(23) (a) Lam, E.; Malkin, R. *FEBS Lett.* **1982**, *44*, 190−199. (b) Lam, E.; Malkin, R. *Proc. Natl. Acad. Sci. U.S.A.* **1982**, *79*, 5494−5498. (c) Lam, E.; Baltimore, B.; Ortiz, W.; Chollar, S.; Melis, A.; Malkin, R. *Biochim. Biophys. Acta* **1983**, *724*, 201−211.

(24) (a) Das, S. K.; Frank, H. A. *Biochemistry* **2002**, *41*, 13087−13095. (b) BBY refers to preparations of PS II particles first described in ref 22.

the sucrose was removed by dialysis in 0.02% β-DM and 10 mM HEPES at pH 7.6. Chl concentrations were measured by methanol extraction using an extinction coefficient of 79.24 mL (mg of Chl)$^{-1}$ cm^{-1} at 665 nm.[25] The reaction center solution contained 6.4 mg of Chl/mL. The prepared intact PS II reaction center was stored at 77 K.

The manganese-depleted PS II was prepared as reported previously.[25] PS II preparations were first subjected to 30 min of incubation with stirring on ice in buffer A [50 mM 2-(*N*-morpholino)ethanesulfonic acid (MES), 15 mM NaCl, 1 mM $CaCl_2$, 5 mM sodium ethylenediaminetetraacetate (Na_4EDTA), 0.4 M sucrose, and 0.03% β-DM at pH 6.5] containing 10 mM hydroxylamine. Hydroxylamine and free manganese ions were removed by two cycles of concentration and resuspension in buffer using an Ultrafree-4 concentrator (Millipore, 100 kDa nominal molecular mass cutoff). Finally, the core complexes were resuspended in a buffer containing 60% glycerol, 50 mM MES, and 0.03% β-DM, and a 100-fold excess of potassium ferricyanide relative to the PS II concentration was added. The prepared PS II reaction center depleted of manganese was concentrated and stored at 77 K.

Characterization of PS II Preparations. The individual proteins in the PS II complexes were dissociated and then subjected to electrophoresis by SDS−PAGE (Supporting Information, Figure S1). Proteins with molecular masses at 47, 43, 33, 23, and 17 kDa were detected in the native PS II sample. In the Mn-depleted PS II, the 47 and 43 kDa proteins were detected, since loss of the Mn cluster causes the proteins with masses 33, 23, and 17 kDa to be lost. These results are characteristic of known native and Mn-depleted PS II proteins from spinach.[22−24]

The presence of the Mn_4 cluster was confirmed by measuring the oxygen evolution rates under visible light illumination using a Clark oxygen electrode (see the Supporting Information). The oxygen evolution activity of the intact PS II samples had an average value of 523 μmol of O_2/(mg of Chl h), consistent with previous studies[22−24] of spinach PS II, indicating that values in excess of 300 μmol of O_2/(mg of Chl h) are characteristic of highly active PS II preparations. For Mn-depleted PS II, the oxygen evolution activity decreased to 93 μmol of O_2/(mg of Chl h), indicating an 82% loss of oxygen evolution activity resulting from the depletion of Mn.

UV−vis spectra (Supporting Information, Figure S2) of dry and wet (pH 6.0 buffer) PS II−lipid films gave characteristic strong absorption bands of the numerous antenna chlorophylls at 680 and 430 nm and were virtually identical to those of native PS II dissolved in pH 6.0 buffer obtained in this and previous work.[26]

Film Preparation and Voltammetry. The techniques used were similar to those reported previously for PS I.[20] Briefly, basal plane pyrolytic graphite disk electrodes (geometric area 0.16 cm^2) were abraded with 600 grit SiC paper and then an emery cloth, then washed with water, and sonicated for 30 s. The electrochemically determined microscopic area obtained from cyclic voltammograms of ferricyanide ion, the known diffusion coefficient, and the Randles−Sevcik equation[27] was $A = 0.21$ cm^2 and was used in surface concentration determinations. Equal volumes of DMPC vesicle dispersions (5.3 mM) and 6.4 mg of Chl/mL of PS II solutions were combined. A 10 μL sample of this dispersion was spread evenly onto rough PG electrodes and dried overnight at 4 °C in the dark. From previous AFM studies of DMPC films with RC proteins,[20] the film thickness is ~2 μm.

Voltammetry was done in a thermostated three-electrode cell (Pt counter, SCE reference) at 4 °C in the dark using a CH Instruments 660A electrochemical analyzer with the ohmic drop compensated by >98%. This low temperature gave the best film stability and reproducibility. All data reported are for repeated scan cyclic voltammograms taken with a ~10 s waiting time after each scan that have become exactly reproducible after several scans. Potentials are reported vs NHE. Buffers were 20 mM MES (pH 6.0) and 20 mM HEPES for pH 7.5 and 8.2, all containing 50 mM NaCl. Solutions were purged with high-purity argon before voltammetry (to remove electroactive oxygen), and an argon/nitrogen atmosphere was maintained above the solutions during the scans. Reproducible voltammograms of DMPC films alone were subtracted from each of the PS II voltammograms, followed by baseline slope correction (for further details, see the Supporting Information, Figures S3−S6).

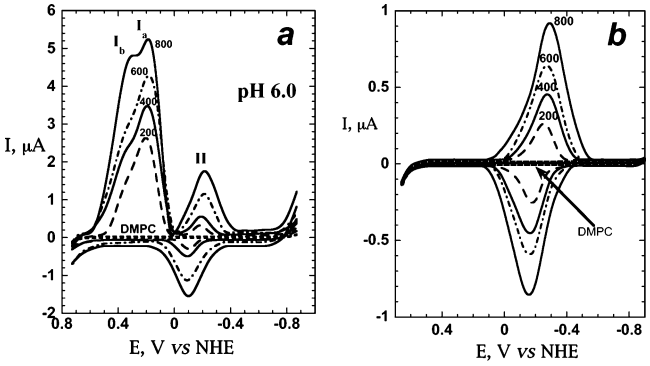

Figure 1. Background-subtracted cyclic voltammograms of spinach PS II RCs in DMPC films in pH 6 MES buffer for (a) native PS II containing the Mn_4 complex and (b) PS II depleted of the Mn_4 complex (scan rates, mV s^{-1}, labeled on the curves; featureless dashed lines represent DMPC films alone).

Results

Cyclic Voltammetry. Steady-state cyclic voltammograms of films made with native PS II and DMPC were obtained in anaerobic buffers of pH 6−8.2. At pH 6, these films gave two peaks, one chemically irreversible and one reversible (Figure 1a). An irreversible reduction peak (I) at low scan rates appeared at 0.21 V (all vs NHE), with a shoulder growing in at about 0.3 V as the scan rates were increased. The second peak system was a well-defined, chemically reversible reduction−oxidation peak pair (II) with a midpoint potential of −0.15 V at low scan rates. DMPC films without PS II were featureless in the potential range of peaks I and II. As mentioned above, UV−vis spectra of PS II−lipid films nearly identical to those of PS II solutions (Figure S2) suggest that PS II remains in a near-native state in the biomimetic film enviroment.

Cyclic voltammograms showed minimal changes over 7 days of storage of PS II−lipid films in buffer in the dark at 4 °C. Repeated cyclic voltammograms were reproducible (±5%), showing no evidence of thinning or decomposition of films on rough PG. Integration of the reduction peak of redox couple II at low scan rates to obtain charge Q and application of Faraday's law ($Q = nF\Gamma_T$) assuming a one-electron ($n = 1$) reaction[10] where F = Faraday's constant gave a surface concentration $\Gamma_T = (1.2 \pm 0.3) \times 10^{-10}$ mol cm^{-2}. The peak current for I and II increased linearly with scan rate up to 800 mV s^{-1}. At scan rates above 1000 mV s^{-1}, the backgrounds became larger and introduced significant uncertainty into the background corrections, so the present study was limited to the lower scan rate range.

Cyclic voltammograms of Mn-depleted PS II in DMPC films gave only a single reversible reduction−oxidation peak pair at potentials corresponding to peak II (Figure 1b). Integrations of this peak revealed a surface concentration of ~0.7×10^{-10} mol

(25) (a) Cheniae, G. M.; Martin, I. F. *Plant Physiol.* **1972**, *50*, 87−94. (b) Tamura, N.; Cheniae, G. M. *Biochim. Biophys. Acta* **1987**, *890*, 179−194. (c) Tracewell, C. A.; Cua, A.; Stewart, D. H.; Bocian, D.; Brudvig, G. *Biochemistry* **2001**, *40*, 193−203.
(26) Brettel, K.; Leibl, W. *Biochim. Biophys. Acta* **2001**, *1507*, 100−114.
(27) Bard, A. J.; Faulkner L. R. *Electrochemical Methods*, 2nd ed.; Wiley: New York, 2002.

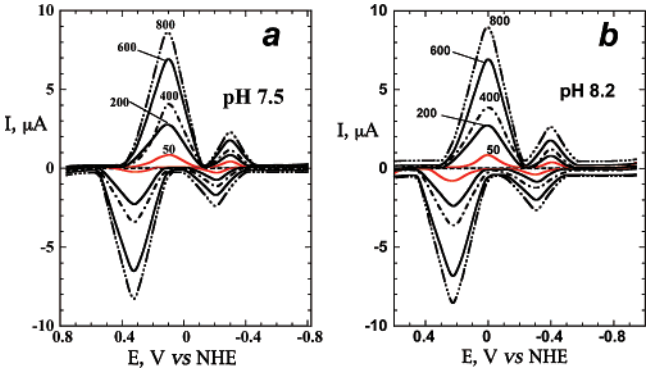

Figure 2. Background-subtracted cyclic voltammograms of intact spinach PS II RCs in DMPC films in HEPES buffer at (a) pH 7.5 and (b) pH 8.2 (scan rates, mV s^{-1}, labeled on the curves; featureless dashed lines represent DMPC films alone).

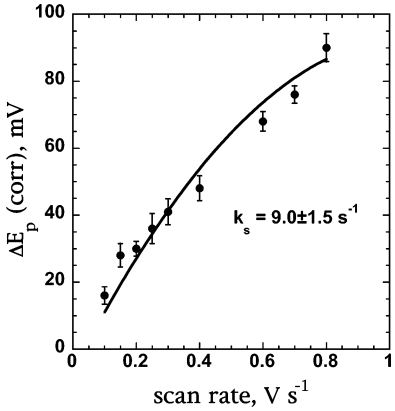

Figure 3. Influence of the CV scan rate for peak II of PS II−DMPC films in pH 6 MES buffer on experimental corrected peak separations (ΔE_p) shown with the theoretical working curve line at $k_s = 9\ s^{-1}$.

cm^{-2}. Peak I (Figure 1a) was absent from these scans, suggesting that the Mn cluster removed from the PS II samples was the cause of peak I in films containing native PS II.

At pH 7.5 and 8.2, peaks I and II shifted negatively, and both redox reactions gave chemically reversible pairs of peaks (Figure 2). At pH 7.5, the midpoint potentials were 0.22 V for peak I and −0.25 V for peak II. At pH 8.2, the midpoint potentials were 0.11 V for peak I and −0.35 V for peak II. All reduction peak heights were linearly proportional to the scan rates, and the peak potentials did not vary with scan rate up to 800 mV s^{-1}.

Curves in red in Figure 2 are cyclic voltammograms at 50 mV s^{-1}. At this low scan rate, the cyclic voltammogram for the peak I system at pH 7.5 is still partly irreversible and shows an oxidation peak that is much smaller than the reduction peak. At higher scan rates or at pH 8.2, the peak I system is always chemically reversible. These results, as well as those at pH 6, are all characteristic of an electron-transfer reaction followed by a chemical deactivation step (EC mechanism),[27] to be discussed later.

At pH 6, oxidation and reduction peak potentials of system II varied in opposite directions with scan rates above 100 mV s^{-1}, with the net effect of increasing the peak separation. These data are consistent with kinetic limitations to electron transfer and are consistent with the Butler−Volmer model for electron transfer between an electrode and redox sites in a thin film on an electrode.[28] Below 100 mV s^{-1} at pH 6, the peak separation was constant. A relatively constant peak separation such as found for redox couple II at low scan rates has been observed in thin films of many redox proteins.[10] It is not related to kinetics, but may result from conformational differences between oxidized and reduced forms of the protein[29] or an N-shaped potential dependence of the reaction coordinate.[30] Following an approach suggested by Hirst and Armstrong,[31] we subtracted this constant peak separation (ΔE_p) at low scan rate and fit these corrected data at higher scan rates to the published working curve for the Butler−Volmer model for electron transfer between the electrode and nondiffusing redox sites.[28] The resulting fit of theory to the corrected ΔE_p vs scan rate was reasonably good and provided an estimate of the apparent electrochemical surface electron-transfer rate constant (k_s) of $9.0 \pm 1.5\ s^{-1}$ (Figure 3).

For all other chemically reversible CV peaks, ΔE_p was constant with scan rate changes or began to vary only at the upper end of the scan rate range. The latter was the case only for peak II at pH 7.5, for which a rough value of 100 s^{-1} was estimated. Thus, 100 s^{-1} represents a lower limit for k_s for the redox processes I and II at pH 7.5 and 8.2.

Square Wave Voltammetry (SWV). Square wave voltammetry has better sensitivity and resolution than CV[32] and has been used to investigate complex processes in protein film voltammetry.[33,34] The pulsed, digital nature of SWV allowed us to access pulse widths as low as 3.3 ms (150 Hz) and still accurately subtract backgrounds. At higher frequencies large background subtractions were necessary and became inaccurate. For native PS II−DMPC films, at pH 6, 7.5, and 8.2, reversible redox forward−reverse peak pairs at potentials corresponding to peaks I and II were observed when the initial potential was 0.7 V and the pulse train scanned toward negative potentials (Figure 4a). In addition, a third smaller peak pair (III) appeared at −0.67 V at pH 6. The peak potentials all shifted negatively with increasing pH, a point we will return to later. The peak potentials of the forward and reverse peaks were equal and did not depend on the frequency or pulse height for all peaks up to 150 Hz and pulse heights to 100 mV at pH 7.5 and 8.2. Small shifts to negative potentials were found for peaks I and III with increasing frequency at pH 6. The peak heights were linearly proportional to the frequency. Thus, all data were consistent with quasireversible or reversible thin film voltammetry[32] for the redox couples under the conditions used. Comparing these data to those of the Butler−Volmer thin film SWV model,[35] the results are consistent with a lower limit on k_s of $\sim 10\ s^{-1}$ for the three redox couples. This is also consistent with the CV result of 9 s^{-1} for the interfacial rate constant obtained for redox couple II.

If the starting potential for SWV was −1.0 V, and the scan direction of the pulse train was toward positive potentials, the

(28) Laviron, E. *J. Electroanal. Chem.* **1979**, *101*, 19−28.
(29) El Kasmi, A.; Leopold, M. C.; Galligan, R.; Robertson, R. T.; Saavedra, S. S.; El Kacemi, K.; Bowden, E. F. *Electrochem. Commun.* **2002**, *4*, 177−181.
(30) Feldberg, S. W.; Rubinstein, I. *J. Electroanal. Chem.* **1988**, *240*, 1−15.
(31) Hirst, J.; Armstrong, F. A. *Anal. Chem.* **1998**, *70*, 5062−5071.
(32) Osteryoung, J.; O'Dea, J. J. In *Electroanalytical Chemistry*; Bard, A. J., Ed.; Marcel Dekker: New York, 1986; Vol. 14, pp 209−308.
(33) Jeuken, L. J. C.; Jones, A. K.; Chapman, S. K.; Cecchini, G.; Armstrong, F. A. *J. Am. Chem. Soc.* **2002**, *124*, 5702−5713.
(34) Jeuken, L. J. C.; McEvoy, J. P.; Armstrong, F. A. *J. Phys. Chem. B* **2002**, *106*, 2304−2313.
(35) (a) Reeves, J. H.; Song, S.; Bowden, E. F. *Anal. Chem.* **1993**, *65*, 683−688. (b) O'Dea, J. J.; Osteryoung, J. *Anal. Chem.* **1993**, *65*, 3090−3097.

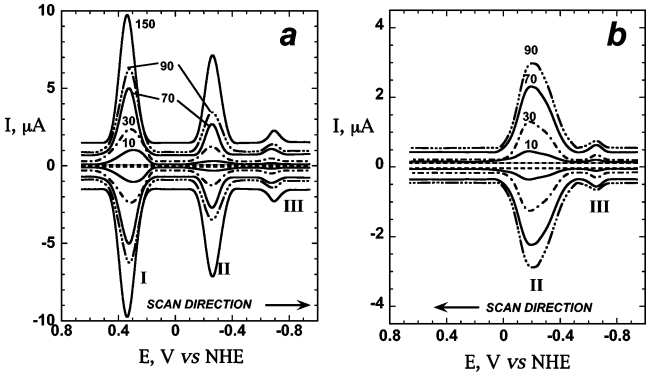

Figure 4. Background-subtracted forward and reverse square wave voltammograms of native spinach PS II RCs in DMPC films at different frequencies in pH 6 MES buffer for (a) a scan in the negative direction and (b) a scan in the positive direction (pulse height 25 mV, step 1 mV, frequency, Hz, labeled on the curves; featureless dashed lines represent DMPC films alone).

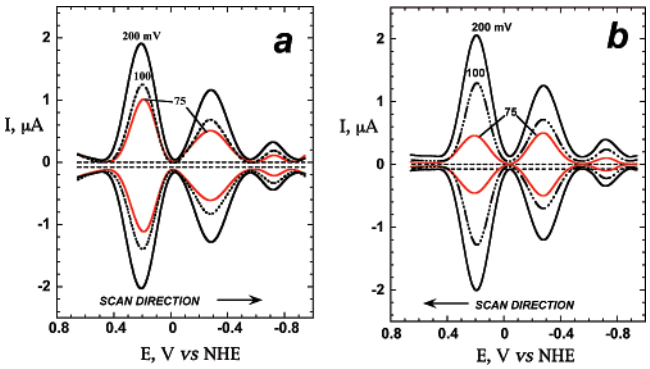

Figure 5. Background-subtracted forward and reverse square wave voltammograms of native spinach PS II RCs in DMPC films at different pulse heights in pH 7.5 HEPES buffer for (a) a scan in the negative direction and (b) a scan in the positive direction (frequency 5 Hz, step 1 mV, pulse height, mV, labeled on the curves; featureless dashed lines represent DMPC films alone).

voltammograms at pH 6 showed only two reversible redox peak pairs (II and III, Figure 4b). Peak I was absent at this pH. At pH 7.5 and 8.2, all three sets of peak pairs were observed independent of the starting potential and direction of scanning (Figure 5). However, changes in these parameters influenced the ratios of peak I to peak II at low frequencies and low pulse heights, illustrated by the red curves in Figure 5. At 5 Hz and a 75 mV pulse height, the peak I/II ratio is ~2 when the scan proceeds negatively but ~0.8 when the scan direction is positive.

SWV of films made with PS II depleted of the manganese cluster showed only reversible couples II and III. The peak I pair was absent. The behaviors of the redox couples II and III at increasing frequencies and pulse amplitude were similar to those obtained from intact PS II.

Peak Potentials. Table 1 lists midpoint potentials for peaks I and II from CV and peak potentials from SWV for peaks I−III, with tentative assignments. Also included are midpoint potentials reported previously in the literature from optical redox titrations of PS II in detergent solutions. Shifts of all peak potentials with pH were linear, and the values of the slopes from SWV are given in Table 2. We consider the E_p vs pH slopes from SWV to be more reliable than those from CV because the midpoint potentials are simply the peak potentials. Values for peaks II and III are consistent with the theoretical value of 54.8 mV pH^{-1} at 4 °C for a one-electron, one-proton electron transfer.[27] The value of 83 for peak I could result from a multielectron, multiproton reaction; e.g., three protons and two electrons gives a theoretical slope of 82.2 mV pH^{-1} at 4 °C.

Table 1. Comparison of Spinach PS II Midpoint Potentials with Literature Values (V vs NHE)

sample	peak I (Mn_4)	peak II [Q/Q^-]	peak III [Pheo/$Pheo^-$]	method
PS II−DMPC	0.2−0.3	−0.15		CV, pH 6.0
PS II−DMPC	0.22	−0.25		CV, pH 7.5
PS II−DMPC	0.11	−0.35		CV, pH 8.2
PS II−DMPC	0.29	−0.25	−0.67	SWV, pH 6.0
PS II−DMPC	0.20	−0.29	−0.72	SWV, pH 7.5
PS II−DMPC	0.10	−0.39	−0.81	SWV, pH 8.2
predicted[11]	0.8−1.2			
PS II dispersion		−0.08, pH 6−7[a] (Q_A)	−0.600,[c] pH 11	spec redox titrations
lit.		−0.3 to +0.07[b]		

[a] From spinach chloroplasts.[36] [b] Range for Q_A for various materials and conditions.[36] [c] From pea chloroplasts.[37]

Table 2. Slopes of Midpoint Potentials vs pH, mV pH^{-1}, for PS II in DMPC Films

method	peak I (Mn_4)	peak II [Q_A/Q_A^-]	peak III [Pheo/$Pheo^-$]
SWV	83	53	59

Discussion

Peak Assignments. The results presented above demonstrate direct, rapid electron transfer between electrodes and cofactors in the PS II reaction center protein embedded in stable biomimetic lipid films. On the basis of studies on smaller proteins in similar films,[13] it is likely that the protein resides spanning hydrophobic regions of the lipid bilayers in the DMPC film in an environment similar to its native one. Cyclic voltammograms (Figure 2) at pH 7.5 and 8.2 gave well-defined, chemically reversible peaks for two redox couples (peaks I and II) in the PS II−DMPC films. At pH 6, only peak II is reversible in CV. At pH 6, 7.5, and 8.2, reversible peaks for three redox couples were observed by SWV (Figures 4 and 5). All of the data for the reversible peaks are consistent with fast electron transfer, with the slowest rate constant k_s being the 9 s^{-1} found for redox couple II at pH 6. The other redox couples as well as couple II at pH 7.5 and 8.2 were consistent with k_s values ≥100 s^{-1}.

Peak I, discussed in more detail below, was assigned to the manganese cluster by virtue of its absence in PS II preparations depleted of manganese (Figure 1b). The other peaks can be tentatively assigned on the basis of comparisons to redox titration values of midpoint potentials from the literature. We cannot expect exact correspondence between values from voltammetry and redox titrations as they are obtained under different experimental conditions and sometimes with different PS II preparations. Also, as we have shown previously for smaller, single-cofactor redox proteins such as myoglobin and cytochrome $P450_{cam}$, potentials from lipid film voltammetry can be shifted by several hundred millivolts by lipid−protein interactions and also depend strongly on the electrode material.[13] These factors may shift the electrochemical redox potential of

(36) Krieger, A.; Rutherford, A.; Johnson, G. *Biochim. Biophys. Acta* **1995**, *1229*, 193−201.
(37) Rutherford, A.; Mullet, J.; Crofts, A. *FEBS Lett.* **1981**, *123*, 235−237.

the manganese cluster in the films well negative of its expected or in vivo midpoint potential (Scheme 1). We did not see any indication of electrochemistry from the P680 center, in either intact or Mn-depleted PS II. P680 resides in a part of the protein different from that where Mn_4 resides and may be subject to different protein−lipid or electrode double-layer interactions that do not shift the potential from its high estimated value (Scheme 1) into a voltammetrically measurable range. Alternatively, the P680 center may simply be insulated from the electrode by the nonelectroactive protein backbone in these films.

Two quinone fractions have been identified in PS II, Q_A at higher potential and Q_B at more negative values in a roughly 2/1 Q_A/Q_B ratio in PS II from peas (Table 1). Values reported in the literature show that the range of reported midpoint potentials is rather wide, but the range corresponds to the values we have obtained by CV and SWV (Table 1). Thus, peak II can be assigned to quinone cofactors.

Accepting this assignment of peak II, the more negative peak III must be assigned to pheophytin because it is the only cofactor in PS II more negative than Q_B (Table 1, Scheme 1). The peak area in protein film voltammetry relates to the charge passed (in CV), the number of electrons in the redox process, the accessibility of the electrode to the redox center, and the amount of protein redox cofactors in the films.[10] Among these factors, the small area of peak III, presumably a one-electron process, may be related to poor accessibility to the electrode or poor electron hopping rates in the film that effectively render a fraction of the cofactor electroinactive.

The midpoint potential−pH slopes for peaks II and III (Table 2) are consistent with theory of 54.8 mV pH^{-1} at 4 °C for a one-electron, one-proton reduction which is in general consistent for quinone and pheophytin electrochemistry.[36,37] However, Q_A midpoint potentials have been reported as both pH-dependent according to a $1e^-/1H^+$ mechanism as we find and pH-independent between pH 5.5 and 7.5.[36]

Manganese Cluster. The electrochemistry presented by peak I and assigned to the manganese cluster is clearly the most intriguing. Peak I in CV at pH 6 is chemically irreversible (Figure 1a) and splits into two overlapping peaks at a higher scan rate. These two overlapping peaks may possibly represent different, competing, proton-coupled oxidation pathways on different time scales within the Mn_4 center. At the higher scan rates, a faster process could predominate. They do not appear in Mn-depleted PS II (Figure 1b). In SWV, the single peak I is reversible for scans to negative potentials begun at 0.7 V, but is clearly absent in positive scans begun at −1 V (Figure 4). In CV at pH 7.5, lower scan rates show a relative decrease in the oxidation peak (Figure 2a, red curve), consistent with electron transfer followed by chemical deactivation, i.e., an EC mechanism (E = electron transfer, C = chemical step).[27] In SWV at pH 7.5 and 8.2, peak I appears, but its relative heights as judged by its ratio to peak II at low frequencies and low pulse heights (red curves in Figure 5) depend on the scan direction. For example, a I/II peak ratio of ∼2 was found for the negative scan at 5 Hz and a 75 mV pulse height, but the positive scan gave a peak ratio of ∼0.8.

Armstrong and co-workers investigated gating of electron transfer by slow preceding deprotonation using thin film voltammetry of a protein and a mutant with buried iron−sulfur clusters.[38,39] They showed with the aid of simulated voltammograms that the disappearance of oxidation peaks in CV in a certain range of scan rates and pH values, as also found for PS II peak I at pH 6 (Figure 1a), was explained by an EC/CE mechanism for reduction−oxidation cycles, respectively. The chemical steps are protonation on the reduction cycle and deprotonation on the oxidation cycle. Thus, at pH 6, we envision the EC reduction process on the forward scan to feature protonation following initial electron transfer (Scheme 2, M = tetramanganese cluster). On the reverse scan, deprotonation must occur to produce M^- for the oxidation to occur (CE mechanism). That is, electron transfer is "gated" by the deprotonation. HM does not appear to be oxidizable in the available potential widow, in agreement with the principle that protonated species are harder to oxidize than the related species that are deprotonated.[27] At pH 6 in CV, deprotonation of HM is slow compared to the time scale, and no oxidation peak is found. At higher pH, it is logical that the protonation rate decreases and the deprotonation rate increases. However, for 50 mV s^{-1} at pH 7.5 (Figure 2a) there is still some chemical irreversibility, as evidenced by an oxidation peak smaller than reduction peak I. Here, protonation occurs, but deprotonation is still slow with respect to the 50 mV s^{-1} time scale. At pH 8.2, where the protonation becomes slower, or at pH 7.5 and scan rates >100 mV s^{-1}, the time scale of the experiment is such that it outruns the protonation, and the reversible cyclic voltammograms (Figure 2) must reflect reversible interconversion of M and M^-, without any slow protonation or deprotonation; i.e., an E/E mechanism pertains.

Scheme 2. EC/CE Process for Manganese Cluster (M) Electrochemistry

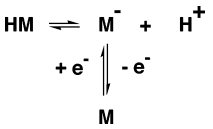

The proton-gated electron-transfer scenario also explains the SWV results. In CV, the scan is continuous and the time scale of a 0.5 V window is about 20 s to 400 ms for our scan rate range of 50−800 mV s^{-1}. The SWV time window, given by the pulse width τ ($\tau = 1/2f$),[32] is 100 to 3.3 ms for the frequencies (f) of 5−150 Hz used. Under the SWV conditions, there is much less time for the slow protonation or deprotonation to occur than in CV. At pH 6, when the starting potential is 0.7 V, the redox couple begins in the oxidized form M. Unlike cyclic voltammetry where there is a continuous scan, the scan in SWV involves movement of a cycle of forward and reverse potential pulses of width τ and of fixed amplitude, in this study 10−100 mV. The square waves are constantly pulsing up and down and sampling the redox state of the reactant at the end of each forward and reverse pulse. Each successive forward−reverse pulse cycle shifts in starting potential by a voltage step, resulting in a "scan" of the pulse waveform. Under these conditions at pH 6, 7.5, and 8, we postulate that protonation of M^- (Scheme 2) never has time to occur within pulse width τ, explaining the fact that the forward and reverse peak pair I is always reversible.

(38) Hirst, J.; Duff, J. L. C.; Jameson, G. N. L.; Kemper, M. A.; Burgess, B. K.; Armstrong. F. A. *J. Am. Chem. Soc.* **1998**, *120*, 7085−7094.
(39) Armstrong, F. A. In *Electroanalytical Methods for Biological Materials*; Chambers, J. Q., Brajter-Toth, A., Eds.; Marcel Dekker: New York, 2002; pp 143−195.

However, when the SWV scan begins at −1 V, the redox couple starts in its protonated, reduced state HM. As the scan proceeds positively, at pH 6 there is never enough time during a single pulse (i.e., within τ) for deprotonation to occur, and no oxidation or reduction peaks are observed. At pH 7.5 and 8, deprotonation is faster and reversible SWV for peak I is again observed, but at low frequency (5 Hz, Figure 5), $\tau = 100$ ms and peak I on the positive scan depends on the pulse amplitude, which is the driving force of the redox process. The electron transfer is now coupled to a deprotonation that has more time to reach equilibrium (100 ms), and if the electrochemical driving force is not large enough, all of the M^- that forms will not be oxidized. Therefore, the peak will be smaller than at larger driving forces (pulse heights) that oxidize all the M^-. There is a coupled LeChatelier equilibrium effect involving electrochemistry and protonation/deprotonation operating here. If some M^- remains unoxidized in the film on the oxidative pulse, it will drive the protonation reaction, but if the driving force is large, that will remove M^- and drive the deprotonation reaction. At a larger pulse amplitude, the ratio of peak I to peak II becomes constant when the chemical and electron-transfer steps are at equilibrium throughout the forward and reverse pulses. When the driving force is too low, as for the 75 mV pulse on the positive scan (Figure 5), the peak height of I is limited by electron-transfer thermodynamics.

The overriding conclusion is that, under conditions where the *reversible* electrochemistry is observed, a nominal E/E reduction−oxidation mechanism occurs in which the experimental time scale is shorter than the gating protonation/deprotonation. Conditions where *chemical irreversibility* occurs appear to foster the proton-gated EC/EC pathway.

However, additional protonations/deprotonations that are too fast to influence peak currents must still control the peak potentials. The pH dependence of peak I in SWV was 83 mV pH^{-1}, which is comparable to the theoretical value of 82.2 mV pH^{-1} at 4 °C for a three-proton/two-electron process. This suggests that there are other fast protonation/deprotonation processes coupled to the overall electrode process. These additional proton transfers are probably fast and at equilibrium during the voltammetry, in agreement with current views of the rates of proton transfer upon photoexcitation of PS II proteins.[40] Only one deprotonation at pH 6 needs to be slow for the mechanistic scenario in Scheme 2 to apply to our voltammetric results.

How can the electrochemical results for peak I be related to the PS II biological function of oxygen evolution? The manganese cluster, also known as the oxygen-evolving complex (OEC), catalyzes oxidation of water to molecular oxygen with the release of four protons and four electrons. According to the classic cycle proposed by Kok,[41] the reaction proceeds through four kinetically resolvable S states (S_0−S_4) of the OEC and oxygen is evolved after every fourth flash of light.

$$2H_2O + 4h\nu \rightarrow O_2 + 4H^+ + 4e^- \qquad (1)$$

These S states have been characterized over the past decade,[42,43] most recently the S_4 state, which features a deprotonation on the 200 μs time scale followed by electron transfer in 1.1 ms to give an S_4' state.[9] A nearby tyrosine (Y_Z) may abstract electrons and protons from the OEC, although an arginine residue has also been proposed for this Y_Z function.[43] Four successive light flashes step the cycle sequentially from S_0 to S_4. Each successive photon results in photoexcitation to give P680*, which oxidizes Y_Z, which then extracts an electron from the manganese complex.

There is no evidence for oxygen evolution from voltammetry. In PS II voltammetry, the electrode donates and extracts electrons from the manganese complex, and it is clear from the pH dependence of the CV and SWV results (Figures 1, 2, 4, and 5 and Tables 1 and 2) that protonations and deprotonations are also involved.[40] Mn-containing model compounds have also shown proton-coupled voltammetry. A tetranuclear Mn^{IV}−adamantine complex, $[Mn_4O_6(bpea)_4ClO_4]_4$, displayed a chemically reversible redox couple at 0.345 V vs NHE corresponding to $Mn_4^{IV,IV,IV,IV}/Mn_4^{III,IV,IV,IV}$ and an irreversible redox peak at $E_m = -0.387$ vs NHE corresponding to $Mn_4^{III,IV,IV,IV}/Mn_4^{III,III,IV,IV}$.[44] A water-soluble form of this tetramanganese complex gave a chemically reversible proton-coupled CV peak at $E_m = 0.301$ mV vs NHE in pH 7 buffer.[44] These studies support the concept of proton-coupled voltammetry in tetramanganese complexes and also show values of midpoint potentials similar to those of our peak I, although our values must be additionally influenced by the protein and film environment. Further, there is model complex evidence that protonation reactions on dimanganese oxo bridges can be slow.[45]

While all four manganese ions in the OEC are needed for efficient oxygen evolution, it has been suggested that only two of them undergo redox changes associated with water oxidation.[46] Proton release accompanying oxygen evolution and manganese oxidation is also important. Most of the deprotonation reactions of the OEC occur in ≤200 μs, e.g., the $S_3 \Rightarrow S_4$ deprotonation described above. Lag phases of 1.2 ms have been identified for the BBY form of PS II associated with $Y_Z^+S_0 \Rightarrow Y_ZS_1$ and $Y_Z^+S_3 \Rightarrow Y_ZS_0$, which presumably are electron-transfer steps. There has been a report of a millisecond release of protons at pH 7.4 and a millisecond uptake of protons at pH 6.3.[40] From the voltammetric data, the deprotonation that is assumed to block oxidation in the peak 1 system at pH 6 is much slower than any of those discussed above, even taking into account the 4-fold increase in the half-time expected per 20° decrease at 4 °C from room temperature, at which most of the existing data have been obtained. At pH 7.5, judging from the CV and SWV data, the deprotonation reaction must occur in ∼100 ms or more. CV data reflecting no deprotonation of the reduced manganese complex at pH 6 (Figure 1a) and partial deprotonation at pH 7.5 and the low scan rate (Figure 2a) suggest a p*K* of ∼7.5 for the species in question. At pH 7.5, a

(40) Lavergne, J.; Junge, W. *Photosynth. Res.* **1993**, *38*, 279−296.
(41) Kok, B.; Forbush B.; McGloin M. *Photochem. Photobiol.* **1970**, *11*, 457−475.
(42) (a) Yachandra, V.; Sauer, K.; Klein, M. *Chem. Rev.* **1996**, *96*, 2927−2950. (b) Ahlbrink, R.; Haumann, M.; Cherepanov, D.; Bogershausen, O.; Mulkidjanian, A.; Junge, W. *Biochemistry* **1998**, *37*, 1131−1142. (c) Wenchuan, L.; Roelofs, T.; Cinco, R.; Rompel, A.; Latimer, M.; Yu, W. Sauer, K.; Klein, M.; Yachandra, V. *J. Am. Chem. Soc.* **2000**, *122*, 3399−3412. (d) Robblee, J.; Messinger, J.; Cinco, R.; McFarlane, K.; Fernandez, C.; Pizarro, S.; Sauer, K.; Klein, M.; Yachandra, V. *J. Am. Chem. Soc.* **2002**, *124*, 7459−7471.
(43) McEvoy, J. P.; Brudvig, G. W. *Phys. Chem. Chem. Phys.* **2004**, *6*, 4754−4763.
(44) Dube, C. E.; Wright, D. W.; Pal, S.; Bonitaebus, P.; Armstrong, W. *J. Am. Chem. Soc.* **1998**, *120*, 3704−3716.
(45) Carroll, J. M.; Norton, J. R. *J. Am. Chem. Soc.* **1992**, *114*, 8744−8745 and references therein.
(46) (a) Renger, G. *Biochim. Biophys. Acta* **2001**, *1501*, 210−228. (b) Renger, G. *Photosynth. Res.* **2003**, *76*, 269−288.

lower limit half-time for deprotonation of ~100 ms suggests a rate constant of ~7 s^{-1} and a protonation rate constant of 2×10^8 M^{-1} s^{-1}. While these values are only rough estimates, the protonation rate is larger than $(0.19-1.1) \times 10^5$ M^{-1} s^{-1} found for oxo-bridged Mn complexes,[45] but smaller than maximum diffusion-controlled rate constants for protonation of acids.[40] The point is that the voltammetric data lead to estimates of on and off rate constants consistent with slow protonation/deprotonation steps.

At the present level of investigation, we can only speculate about the site of the deprotonation. Possibilities include protons on oxo bridges, which can be expected to have inherently slow kinetics, or a site that is somehow sequestered from bulk water. Also, the extent to which deprotonation rates may be mediated by the lipid environment of PS II in the film is not known. While lipid films are known to contain significant amounts of water between their stacked bilayers,[13] it is possible that the manganese center resides in a hydrophobic location that does not have full access to water. A further complication is the phase of the films. DMPC films have a gel-to-liquid crystal phase transition temperature of 25 °C[47] and at 4 °C exist in the solidlike gel phase. Such an environment for PS II may further inhibit the key deprotonation during voltammetry compared to those in detergent dispersions at room temperature that are commonly used for such measurements. These and other questions about PS II voltammetry are under further investigation.

In summary, pairs of direct electron-transfer peaks were found in thin film cyclic and square wave voltammetry, reflecting reversible redox couples of PS II in lipid films and assigned to the Mn cluster, quinones, and pheophytin. The redox couples show fast, reversible electron transfer under many conditions. However, on time scales ≥100 ms in voltammetry at pH 6, the manganese cluster oxidation appears to be gated by slow deprotonation of a reduced form.

Acknowledgment. This work was supported by the U.S. Department of Agriculture (USDA) through Grant No. 2002-35318-12484. We thank Gary Brudvig of Yale University for advice on BBY preparation and for oxygen evolution measurements.

Supporting Information Available: Seven additional figures illustrating gel electrophoretic analysis of PS II materials, text describing the results of oxygen evolution from PS II materials, UV−vis spectra of PS II−DMPC films, examples of background subtraction for voltammograms, and SWV of PS II−DMPC films. This material is available free of charge via the Internet at http://pubs.acs.org.

JA0645537

(47) Nassar, A.-E. F.; Zhang, Z.; Rusling, J. F.; Chynwat, V.; Frank, H. A.; Suga. K. *J. Phys. Chem. B* **1995**, *99*, 11013−11017.